Modeling of thermal oxidation of silicon [Erratum to document cited in CA109(14):116856g]

ARTICLE *in* INDUSTRIAL & ENGINEERING CHEMISTRY RESEARCH · JULY 1989

Impact Factor: 2.59 · DOI: 10.1021/ie00091a039

4 AUTHORS, INCLUDING:

Satish K Singh

Pfizer Inc.

85 PUBLICATIONS **1,619** CITATIONS

SEE PROFILE

John R. Schlup

Kansas State University

46 PUBLICATIONS **780** CITATIONS

SEE PROFILE

Biswajit Sur

Allvia

7 PUBLICATIONS **37** CITATIONS

SEE PROFILE

Nomenclature

A = parameter defined in eq 4
A_0 = parameter defined in eq 4
A_1 = parameter defined in eq 4
B = parameter defined in eq 5
C = concentration, kmol/m^3
C_p = heat capacity, J/(kmol·K)
D = diffusivity, m^2/s
D_E = eddy diffusivity, m^2/s
d = reactor diameter, m
f = friction coefficient, dimensionless
g = acceleration of gravity, m/s^2
ΔH_R = reaction enthalpy, J/kmol
h_G = gas-to-liquid heat-transfer coefficient, J/(m^2·s·K)
h_w = wall to refrigerated water heat-transfer coefficient, J/(m^2·s·K)
K_L = liquid thermal conductivity, J/(m·s·K)
K_w = wall thermal conductivity, J/(m·s·K)
K_G = gas-phase mass-transfer coefficient, m/s
k = reaction rate constant, m^3/(kmol·s)
L = reactor length, m
m = SO_3 Henry's constant, (kmol of SO_3/m^3 of gas)/(kmol of SO_3/m^3 of liquid)
N = absorption rate per unit of area, kmol/(m^2·s)
r = reaction rate, kmol/(m^3·s)
T = temperature, K
U = gas mean velocity, m/s
U_L = global heat-transfer coefficient, J/(m^2·s·K)
u = gas velocity, m/s
u_0 = turbulence characteristic velocity of gas, m/s
V = liquid mean velocity, m/s
v = liquid velocity, m/s
X = conversion, dimensionless
y = transversal coordinate, m
y^+ = dimensionless transversal coordinate, yu_0/ν
z = axial coordinate, m

Greek Symbols

α = thermal diffusivity, m^2/s
α_E = eddy thermal diffusivity, m^2/s
Γ = flow per perimeter unit, m^2/s
ϕ = dimensionless function defined in eq 19
δ = film thickness, m
δ^+ = dimensionless film thickness, $\delta u_0/\nu$
μ = dynamic viscosity, kg/(m·s)
ν = kinematic viscosity, m^2/s
ρ = density, kg/m^3
τ = interfacial shear stress, Pa

Subscripts and Superscripts

E = eddy
ex = exterior
G = in gas phase
i = in the interface
in = interior
L = in liquid phase
lm = logarithmic mean
R = of the refrigerated water
w = in the wall

Registry No. Dodecylbenzene, 123-01-3.

Literature Cited

Bird, R. B.; Steward, W. E.; Lightfoot, E. N. *Transport Phenomena*; Wiley: New York, 1960.
Brönstrom, A. *Trans. Inst. Chem. Eng.* **1975**, *53*, 29.
Cook, R. A.; Reginald, H. C. *Ind. Eng. Chem. Fundam.* **1973**, *12*, 106.
Davies, J. T. *Turbulence Phenomena*; Academic: New York, 1972.
Davis, E. J.; David, M. M. *Ind. Eng. Chem. Fundam.* **1964**, *3*, 111.
Davis, E. J.; Ouwerkerk, M. V.; Venkatesh, S. *Chem. Eng. Sci.* **1979**, *34*, 539.
Gilliland, E. R.; Sherwood, T. K. *Ind. Eng. Chem.* **1934**, *26*, 516.
Henstock, V. H.; Hanratty, T. J. *AIChE J.* **1979**, *25*, 122.
Himmelblau, D. M. *Process Analysis by Statistical Methods*; Wiley: New York, 1970.
Jepsen, J. C.; Crosser, O. K.; Perry, R. H. *AIChE J.* **1966**, *12*, 186.
Johnson, G. R.; Crynes, B. L. *Ind. Eng. Chem. Process Des. Dev.* **1974**, *13*, 6.
Lapidus, L. *Digital Computation for Chemical Engineers*; McGraw-Hill: New York, 1962.
Levich, V. G. *Physicochemical Hydrodynamics*; Prentice-Hall: Englewood Cliffs, NJ, 1962.
Mann, R.; Moyes, H. *AIChE J.* **1977**, *23*, 17.
Mann, R.; Knish, P.; Allan, J. C. *ACS Symp. Ser.* **1982**, *196*, 1.
McReady, M. J.; Hanratty, T. J. In *Gas Transfer at Water Surfaces*; D. Reidel: Dordrecht, Holland, 1984.
Pierson, F. W.; Whitaker, S. *Ind. Eng. Chem. Fundam.* **1977**, *16*, 401.
Reid, R. C.; Prausnitz, J. M.; Sherwood, T. K. *The Properties of Gases and Liquids*; McGraw-Hill: New York, 1977.
Yih, S.; Liu, J. *AIChE J.* **1983**, *29*, 903.

Received for review April 9, 1987
Revised manuscript received January 6, 1988
Accepted February 8, 1988

Modeling of Thermal Oxidation of Silicon

Satish K. Singh,[†‡] John R. Schlup,*[†] L. T. Fan,[†] and Biswajit Sur[§]
Department of Chemical Engineering and Department of Mechanical Engineering, Durland Hall, Kansas State University, Manhattan, Kansas 66506

The thermal oxidation of silicon is a standard process step in the fabrication of integrated circuits. A generalized one-dimensional model for dry oxidation of silicon has been derived; it takes into account simultaneous heat and mass transfer. A simplified version of the model has been solved to predict the growth of the oxide layer as a function of reaction temperature. The predicted values are in good agreement with experimental observations. The model also enables the prediction of temperature gradients at the Si–SiO_2 interface, along with approximate temperature profiles in the Si and SiO_2 regions. Temperature gradients have been found to be insignificant for the Si–SiO_2 dry oxidation system.

The thermal oxidation of silicon is a standard process step in the fabrication of modern integrated circuits (IC's). Production of high-quality IC's requires not only an understanding of the basic oxidation mechanism, but also the ability to form a high-quality oxide in a controlled and repeatable manner. Silicon dioxide has several uses: to serve as a mask against implantation or diffusion of dopants into silicon, to provide surface passivation, to isolate (dielectrically) one device from another, to act as a com-

* Author to whom correspondence should be addressed.
† Department of Chemical Engineering.
‡ Current address: ACO Läkemedel AB, 17103 Solna, Sweden.
§ Department of Mechanical Engineering.

0888-5885/88/2627-1707$01.50/0

ponent in MOS structures, and to provide electrical isolation of multilevel metallization systems. Several techniques for forming the oxide layers have been developed, including thermal oxidation, wet anodization, vapor-phase deposition, and plasma anodization or oxidation. Among these techniques, thermal oxidation (using dry oxygen or steam) is the principal technique employed in IC processing (Katz, 1983).

Owing to its importance, thermal oxidation of silicon has been studied extensively, and a large number of experimental data are available (see, e.g., Deal and Grove (1965) and references therein, Katz (1983), and Ghandhi (1983)). Analysis of the growth of the oxide layer in this process has conventionally resorted to a steady-state diffusion model originally presented by Deal and Grove in 1965 (see, e.g., Katz (1983)). If the flux of oxidant through the boundary layer and the surface oxide layer to the reaction rate at the Si–SiO_2 interface are equated, a mixed parabolic relationship is obtained between the thickness of oxide layer and the physicochemical constants of the system. The model is purely correlative in nature and generally valid for temperatures in the range between 700 and 1300 °C, partial pressures between 0.2 and 1.0 atm, and oxide thicknesses between 300 and 20 000 Å, with oxygen and steam ambients. The model assumes a uniform temperature profile within the system. This results in a negligible rate of heat transport within the system and neglect of any thermal effects due to the heat of reaction at the interface.

A model based on the integral mass conservation equation to describe the moving boundaries in the oxidation system has been presented by Dutton and Antoniadis (1978). An accurate representation of induced interfacial fluxes was made and a numerical algorithm presented. However, this model has not been applied to the prediction of oxide layer thickness. Moreover, heat-transfer effects are not included in the model.

The dry oxidation of silicon is highly exothermic (~215 kcal mol^{-1}). This is sufficient to raise the temperature of a silicon cube having a volume of 10^{-6} m^3 above its melting point. Therefore, caution should be used in neglecting the heat-transfer effects in modeling dry oxidation of silicon.

A rigorous one-dimensional model for the dry oxidation of silicon is reported herein. The model includes the effects of mass and heat transfer and of the density changes upon formation of the SiO_2 layer. A numerical solution has been obtained to predict the rate of oxide film growth and the temperature profiles in the system. These growth rates are then compared with experimental data. The model is general and can be applied to heterogeneous gas–solid reactions with the reaction occurring at a moving interface.

Derivation

A scheme of the system modeled in this work is shown in Figure 1. It consists of a thin silicon wafer (thickness ≪ length or width) inserted in a dry oxidation chamber maintained at a specific temperature and pressure. The system under consideration corresponds to the situation where the wafer is oxidized on both faces, in which case the origin in Figure 1 lies along the axis of symmetry.

The silicon surface has a high affinity for oxygen; an oxide layer is formed "rapidly" when it is exposed to an oxidizing ambient. The chemical reaction occurring at the Si–SiO_2 interface in dry oxidation is

$$Si(s) + O_2(g) \rightarrow SiO_2(s)$$

During the course of oxidation, the Si–SiO_2 interface moves into the silicon; however, the volume of the oxide layer expands, resulting in the external SiO_2 surface not being coplanar with the original silicon surface. The oxidation

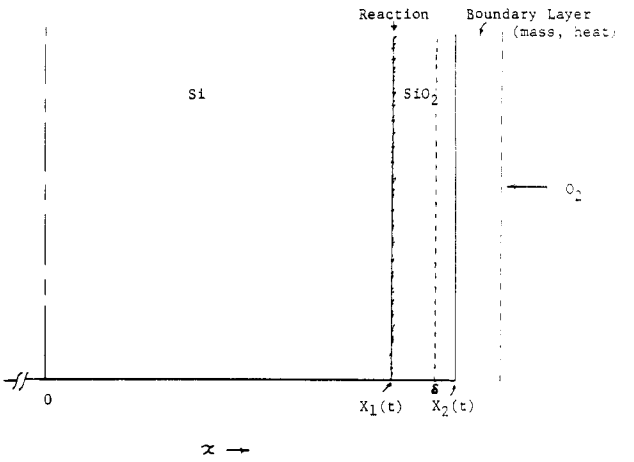

Figure 1. Scheme of the system under consideration.

proceeds by the diffusion of the oxidizing species through the oxide to the Si–SiO_2 interface, where reaction occurs. The thickness of the Si–SiO_2 interface is assumed to be negligible. It is assumed that the oxidizing species is consumed completely at the Si–SiO_2 interface which implies that transport of the oxidizing species into the silicon region is negligible. Some controversy exists as to whether charged (O_2^- or O_2^{2-}) or neutral O_2 species are transported through the oxide film. For the purpose of the present derivation, transport of a neutral species is assumed; however, transport of a charged species can be easily accommodated by the addition of a convective (drift) term to the diffusion equations (see, e.g., Yariv (1982)).

Transport of O_2 in the Oxide Layer. In the oxide region where $X_1^+ \leq x \leq X_2^-$ and for $t > 0$, a mass balance on a shell of unit cross-sectional area and thickness Δx is given by

$$\frac{\partial C}{\partial t} = \frac{\partial}{\partial x}\left(D\frac{\partial C}{\partial x}\right) - \frac{\partial}{\partial x}(V_2 C) \tag{1}$$

where the (convective) velocity of the oxide layer (due to volumetric expansion) is V_2. At time $t = 0$, the thickness of the oxide layer is zero; i.e.,

$$X_1(0) = X_2(0) = \delta \tag{2}$$

The flux continuity of the diffusing species at the SiO_2–boundary layer interface at X_2 leads to the boundary condition

$$-D\left.\frac{\partial C}{\partial x}\right|_{x=X_2^-} = -h_m[C^*(T_o) - C]|_{x=X_2} \tag{3}$$

A mass balance on the oxidizing species at the Si–SiO_2 interface yields

$$\left[-D\frac{\partial C}{\partial x} + V_2 C\right]_{x=X_1^+} = -k''C|_{x=X_1} \tag{4}$$

Transport of Heat in the Silicon Layer. In the region $0 \leq x \leq X_1^-$ and for $t \geq 0$, the unsteady-state heat-transport equation is simply

$$\partial T_s/\partial t = \alpha_s\, \partial^2 T_s/\partial x^2 \tag{5}$$

For simplicity, the temperature and position dependence of the thermal conductivity and density of the silicon layer are neglected (Bird et al., 1960). There is no convective (volumetric expansion) term in this region since the region is stationary with respect to the origin. The initial temperature distribution in the wafer is given by

$$T_s(x,0) = T_I(x) \tag{6}$$

The first boundary condition

$$-K_s \left.\frac{\partial T_s}{\partial x}\right|_{x=0} = 0 \tag{7}$$

implies that no transport occurs across the center of the wafer. At the Si–SiO_2 interface, the two layers are at the same (reaction) temperature:

$$T_s(x=X_1^-,t) = T_o(x=X_1^+,t) \equiv T_r(t) \tag{8}$$

Transport of Heat in the Oxide Layer. The governing equation for heat transport in the region $X_1^+ \leq x \leq X_2^-$ is similar to the mass-transport equation and is given by

$$\frac{\partial T_o}{\partial t} = \alpha_o \frac{\partial^2 T_o}{\partial x^2} - \frac{\partial}{\partial x}(V_o T_o) \tag{9a}$$

As a first approximation, the temperature dependencies of the thermal conductivity and of the density of the silicon dioxide layer have been neglected. In the above equation, V_o is the convective velocity for heat transfer in the oxide region and includes contributions from the volumetric expansion of the oxide region due to Si–SiO_2 conversion, V_2, and the transport of oxygen in this region. Therefore,

$$V_o(x,t) = V_2 + \frac{\left(-D\frac{\partial C}{\partial x} + V_2 C\right) M_g C_{pg}}{\rho_o C_{po}} \tag{9b}$$

The heat flux continuity at the SiO_2–boundary layer interface at X_2 leads to

$$-K_o \left.\frac{\partial T_o}{\partial x}\right|_{x=X_2^-} = -h_t(T_G - T_o)|_{x=X_2} \tag{10}$$

Finally, the continuity of fluxes on both sides of the Si–SiO_2 interface gives rise to the jump heat balance

$$\left[-K_s \frac{\partial T_s}{\partial x}\right]_{X_1^-} - \left[-K_o \frac{\partial T_o}{\partial x} + V_o \rho_o C_{po} T_o\right]_{X_1^+} =$$

$$(\rho_s C_{ps} T_s - \rho_o C_{po} T_o)_{X_1} V_1(t) - [|\Delta H| k'' C]_{X_1} \tag{11}$$

$V_1(t)$ is the velocity of the Si–SiO_2 interface and is proportional to the rate of conversion of Si to SiO_2; i.e.,

$$V_1(t) = -\frac{M_s}{\rho_s} k'' C|_{x=X_1} \tag{12}$$

The velocity of the SiO_2–boundary layer interface, $V_2(t)$, and the velocity of the Si–SiO_2 interface, $V_1(t)$, can be related by a mass balance yielding

$$V_2(t) = (1-\gamma) V_1(t) \tag{13}$$

where

$$\gamma = \frac{\rho_s/M_s}{\rho_o/M_o} \tag{14}$$

The temperature dependencies of some of the physicochemical parameters utilized in the above derivation are given in the Appendix.

The system of governing differential equations and boundary conditions can be converted to dimensionless forms. Due to the orders-of-magnitude difference in the thicknesses of the silicon and oxide layers, different factors are used to nondimensionalize the spatial coordinate in these regions; i.e.,

$$z_s = x/\delta, \quad 0 \leq x \leq X_1^-: \text{ silicon region} \tag{15a}$$

$$z_o = x/\delta_o, \quad X_1^+ \leq x \leq X_2^-: \text{ oxide region} \tag{15b}$$

where δ/δ_o is of the order of 1000. Fourier time is used for the temporal coordinate; it is defined as

$$\tau = D_0 t/\delta_o^2 \tag{15c}$$

The remaining dimensionless groups are listed in the Nomenclature section.

The governing equations, eq 1, 5, and 9, can now be rewritten, respectively, as

$$\frac{\partial y}{\partial \tau} = \frac{\partial}{\partial z_o}\left[\exp(-A_d/\theta_o)\frac{\partial y}{\partial z_o}\right] - \left[\frac{dZ_2}{d\tau}\right]\frac{\partial y}{\partial z_o}$$

$$Z_1^{o+} \leq z_o \leq Z_2^o \quad \tau > 0 \tag{16}$$

$$\frac{\partial \theta_s}{\partial \tau} = \eta^2 R_s \frac{\partial \theta_s}{\partial z_s} \qquad 0 \leq z_s \leq Z_1^{s-} \quad \tau \geq 0 \tag{17}$$

$$\frac{\partial \theta_o}{\partial \tau} = R_o \frac{\partial^2 \theta_o}{\partial z_o^2} - \frac{\partial}{\partial z_o}(U_o \theta_o) \tag{18}$$

The initial conditions, eq 2 and 6, in dimensionless form are

$$Z_1^o(0) = Z_2^o(0) = 1/\eta \tag{19}$$

$$\theta_s(z_s,0) = \theta_I(z_s) \tag{20}$$

The nondimensional boundary conditions, corresponding to eq 3, 4, 7, 8, 10, and 11, are, respectively,

$$\left[\exp(-A_d/\theta_o)\frac{\partial y}{\partial z_o}\right]_{Z_2^{o-}} = Nu_m[y^*(\theta_o) - y]|_{Z_2^o} \tag{21}$$

$$\left[-\left(\exp(-A_d/\theta_o)\frac{\partial y}{\partial z_o}\right) + \left[\frac{dZ_2^o}{d\tau}\right]y\right]_{Z_1^{o+}} =$$

$$-S_r \exp(-A_r/\theta_r) y|_{Z_1^o} \tag{22}$$

$$\left.\frac{\partial \theta_s}{\partial z_s}\right|_0 = 0 \tag{23}$$

$$\theta_s(Z_1^{s-},\tau) = \theta_o(Z_1^{o+},\tau) \equiv \theta_r(\tau) \tag{24}$$

$$\left.\frac{\partial \theta_o}{\partial Z_o}\right|_{Z_2^{o-}} = Nu_{ho}(\theta_G - \theta_o)|_{Z_2^o} \tag{25}$$

$$\left[-\eta R_{so}\frac{\partial \theta_s}{\partial z_s}\right]_{Z_1^{s-}} - \left[-\frac{\partial \theta_o}{\partial z_o} + \frac{U_o \theta_o}{R_o}\right]_{Z_1^{o+}} =$$

$$\theta_r\left(\frac{R_{so}}{R_s} - \frac{1}{R_o}\right)\left[\frac{dZ_1^o}{d\tau}\right] - [H \exp(-A_r/\theta_r) y]_{Z_1^o} \tag{26}$$

Equations 12 and 13 can be rewritten, respectively, as

$$[dZ_1^o/d\tau] = -S_r W \exp(-A_r/\theta_r) y|_{Z_1^o} \tag{27}$$

$$[dZ_2^o/d\tau] = (1-\gamma)\left[\frac{dZ_1^o}{d\tau}\right] \tag{28}$$

Simplifications and Solution

The system of governing equations derived above is a set of nonlinear partial differential equations coupled through the dependency of the reaction term on both concentration and temperature. The regions over which the equations are valid are functions of time. Numerical methods, even for the simplest case of pure heat transfer with a moving boundary, are generally difficult and complicated (see, e.g., Tao (1967), Dutton and Antoniadis (1978), and Talmon et al. (1981)). However, the problem at hand has certain features making it even more difficult. The first is its nonlinearity. The second is the nonexistence of the oxide region at time zero, which results in a singu-

larity in the system (see, e.g., Crank (1957) for a treatment of such a singularity; also see Singh and Fan (1986)). Finally, the "stiffness" of the system due to the widely different time constants of the rate processes under consideration is a very important aspect of the problem. Estimates from experimental data (Deal and Grove, 1965) for the rates of the processes involved in thermal oxidation of silicon show that, at 1273 K, the rate of growth of oxide film is $\sim 10^{-8}$ cm/s, the reaction rate is $\sim 10^{-3}$ cm/s, the diffusive mass-transfer rate (diffusivity/thickness) is $\sim 10^{-5}$ cm/s, the boundary layer mass-transfer rate is ~ 3 cm/s, and the heat-transfer rate (thermal diffusivity/thickness) in oxide is ~ 10 cm/s and in silicon is ~ 2 cm/s.

These widely different rates permit some simplifications to be made. The most obvious simplification would be to neglect temperature gradients in the system (as is done in conventional treatments). However, this would negate the object of the present study. Instead, a pseudo-steady-state assumption for the temperature profile in the oxide layer will be invoked in this study. Under this assumption, the temperature in the oxide layer attains its steady-state (though nonuniform) profile at any instant with respect to the concentration profile and the position of the $Si-SiO_2$ interface. However, no such assumption will be imposed on the temperature in the silicon region (silicon layer:oxide layer, 200:1 to 1000:1); i.e., the unsteady-state temperature profile will be calculated in this region. Thermal gradients within the system have been completely neglected in more conventional treatments.

Furthermore, the relatively thin oxide layer will have a very small volumetric expansion rate; the convective terms, $[dZ_2^\circ/d\tau]$ and $U_o(z_o,\tau)$, arising from this expansion can, therefore, be neglected in the transport equations. With these simplifications, the steady-state version of eq 18, along with eq 24, yields the solution

$$\theta_o(z_o,\tau) = \mathcal{P} z_o + \mathcal{Q} \tag{29}$$

where

$$\mathcal{P} = \frac{\theta_o(Z_2^\circ,\tau) - \theta_r(\tau)}{Z_2^\circ - Z_1^\circ} \tag{30a}$$

and

$$\mathcal{Q} = \frac{\theta_r(\tau) Z_2^\circ - \theta_o(Z_2^\circ,\tau) Z_1^\circ}{Z_2^\circ - Z_1^\circ} \tag{30b}$$

In the above equations,

$$\theta_r(\tau) \equiv \theta_o(Z_1^\circ,\tau)$$

Substituting this solution into eq 25 and rearranging yields

$$\theta_o(Z_2^\circ,\tau) = \frac{\theta_r(\tau) + Nu_{ho}(Z_2^\circ - Z_1^\circ)\theta_G}{1 + Nu_{ho}(Z_2^\circ - Z_1^\circ)} \tag{31}$$

Substituting this expression back into eq 30a and 30b provides the solution for $\theta_o(z_o,\tau)$ in terms of $\theta_r(\tau)$, θ_G, Z_2°, and Z_1°.

The diffusive mass-transfer rate is slow in comparison with the heat-transfer rate. Therefore, it is possible to solve eq 16 (after dropping the convective term, as discussed earlier) under the pseudo-steady-state assumption that θ_o does not depend on z_o and τ, and Z_2° and Z_1° are invariant; this gives (see, e.g., Wen (1968) and Rubinstein (1971))

$$y(z_o,\tau) = y_2 + (y_1 - y_2)\frac{\mathrm{erf}[(Z_2^\circ - z_o)/2(\exp(-A_d/\theta_o)\tau)^{1/2}]}{\mathrm{erf}[(Z_2^\circ - Z_1^\circ)/2(\exp(-A_d/\theta_r)\tau)^{1/2}]} \tag{32}$$

where the following notation has been adopted for conciseness:

$$y_1 \equiv y(Z_1^\circ,\tau) \tag{33a}$$

$$y_2 \equiv y(Z_2^\circ,\tau) \tag{33b}$$

Substituting this solution into eq 21 and 22 gives two simultaneous equations for y_1 and y_2. These may, in turn, be solved algebraically, thereby giving

$$y_1 = \frac{\mathcal{A}\mathcal{D}S_m y^*(\theta_o|_{Z^\circ})_2}{\mathcal{B}\mathcal{E} + (\mathcal{A}\mathcal{D} + \mathcal{C}\mathcal{E})Nu_m} \tag{34}$$

where

$$\mathcal{A} = (\exp(-A_d/\theta_r)/\pi\tau)^{1/2} \tag{35a}$$

$$\mathcal{B} = (\exp(-A_d/\theta_o|_{Z_2^\circ})/\pi\tau)^{1/2} \tag{35b}$$

($\theta_o|_{Z_2^\circ}$ may be obtained from eq 31.)

$$\mathcal{C} = \mathrm{erf}[(Z_2^\circ - Z_1^\circ)/2(\exp(-A_d/\theta_r)\tau)^{1/2}] \tag{35c}$$

$$\mathcal{D} = \exp[-(Z_2^\circ - Z_1^\circ)^2/4\exp(-A_d/\theta_r)\tau] \tag{35d}$$

$$\mathcal{E} = S_r \exp(-A_r/\theta_r) \tag{35e}$$

and

$$y_2 = \frac{CNu_m y^*(\theta_o|_{Z_2^\circ}) + \mathcal{B}y_1}{CNu_m + \mathcal{B}} \tag{36}$$

At this point, the unsteady-state temperature profile in the silicon region $[\theta_s(z_s,\tau)]$ may be obtained in terms of the unknown $\theta_r(\tau)$ by solving eq 17 analytically, subject to eq 20, 23, and 24. This requires the assumption that the $Si-SiO_2$ interface is immobile at any instant with respect to the heat-transfer process (the previous assumption of pseudo-steady-state conditions for the temperature profile). The estimates of oxide film growth rate and heat-transfer rate given earlier show this assumption to be reasonable. When this analytical solution is substituted back into eq 26 and eq 29 is utilized, an expression would be obtained for $[d\theta_r/d\tau]$ in terms of θ_r, $y|_{Z_1^{o+}}$ and τ. This could conceivably be solved in conjunction with eq 34. Nevertheless, the solution for $\theta_s(z_s,\tau)$ would be in terms of an infinite summation, and the resultant expression for $[d\theta_r/d\tau]$ would, therefore, be an integrodifferential (albeit ordinary) equation (along with the infinite summation).

One final simplification is made by assuming that the solution for a semiinfinite bar may be utilized for the silicon region. While the thickness of the silicon layer is on the order of 1 cm or less, the assumption of a semiinfinite bar is reasonable in light of the relative thicknesses of the oxide and silicon layers (silicon:oxide, 200:1 to 1000:1). Solution of eq 17 on a semiinfinite bar, subject to eq 20 and 24, is (see, e.g., Carslaw and Jaeger, (1959))

$$\theta_s(z_s,\tau) = \frac{2}{\pi^{1/2}}\int_{(Z_1^s - z_s)/(2\eta(R_s\tau)^{1/2})}^{-\infty} \theta_r\left[\tau - \frac{(Z_1^s - z_s)^2}{4\eta^2 R_s u^2}\right] e^{-u^2}\,du + \theta_I\,\mathrm{erf}\left(\frac{Z_1^s - z_s}{2\eta(R_s\tau)^{1/2}}\right) \tag{37}$$

Taking the derivative of the above expression with respect to z_s and then the limit as $z_s \to Z_1^{s-}$, we obtain

$$\left.\frac{\partial\theta_s}{\partial z_s}\right|_{Z_1^{s-}} = \frac{2}{\eta}\left(\frac{\tau}{\pi R_s}\right)^{1/2}\frac{d\theta_r}{d\tau} \tag{38}$$

Similarly, taking the direction of $\theta_o(z_o,\tau)$ with respect to

z_o evaluated at Z_1^{o+} (from eq 29), we have

$$\left.\frac{\partial\theta_o}{\partial z_o}\right|_{Z_1^{o+}} = \frac{[\theta_G - \theta_r(\tau)]Nu_{ho}}{1 + Nu_{ho}(Z_2^o - Z_1^o)} \tag{39}$$

Substituting eq 38 and 39 into the boundary condition, eq 26, gives rise to the following nonlinear ordinary differential equation in θ_r:

$$\frac{d\theta_r}{d\tau}\left\{-2R_{so}\left(\frac{\tau}{\pi/R_s}\right)^{1/2}\right\} - \theta_r\left\{\frac{Nu_{ho}}{1 + Nu_{ho}(Z_2^o - Z_1^o)} + \left(\frac{R_{so}}{R_s} - \frac{1}{R_o}\right)\left[\frac{dZ_1^o}{d\tau}\right]\right\} + \left\{\frac{\theta_G Nu_{ho}}{1 + Nu_{ho}(Z_2^o - Z_1^o)} + [H\exp(-A_r/\theta_r)y]_{Z_1^o}\right\} = 0 \tag{40}$$

The above differential equation is of the form

$$\frac{d\theta_r}{d\tau}[-\mathcal{F}(\tau)^{1/2}] - \theta_r\mathcal{G} + \mathcal{H} = 0$$

and can be solved formally, by direct integration. The following solution is obtained:

$$\theta_r(\tau) = \frac{\mathcal{H}}{\mathcal{G}} - \left(\frac{\mathcal{H}}{\mathcal{G}} - \theta_I\right)\exp(-2\mathcal{G}\tau^{1/2}/\mathcal{F}) \tag{41}$$

where

$$\mathcal{F} = 2R_{so}(1/\pi R_s)^{1/2} \tag{42a}$$

$$\mathcal{G} = \frac{Nu_{ho}}{1 + Nu_{ho}(Z_2^o - Z_1^o)} + \left(\frac{R_{so}}{R_s} - \frac{1}{R_o}\right)\left[\frac{dZ_1^o}{d\tau}\right] \tag{42b}$$

and

$$\mathcal{H} = \frac{\theta_G Nu_{ho}}{1 + Nu_{ho}(Z_2^o - Z_1^o)} + [H\exp(-A_r/\theta_r)y]_{Z_1^o} \tag{42c}$$

The nonlinearities in the differential equation will be accounted for through the iterative solution procedure discussed below. The description of $[dZ_1^o/d\tau]$ in terms of $y|_{Z_1^o}$ (from eq 34) still holds; thus,

$$[dZ_1^o/d\tau] = -S_r W\exp(-A_r/\theta_r)y|_{Z_1^o} \tag{27}$$

while

$$Z_1^o(\tau) = Z_1^o(0) + \int_0^\tau \left[\frac{dZ_1^o}{d\tau}\right]d\tau \tag{43}$$

and

$$Z_2^o(\tau) = \frac{\gamma}{\eta} + (1 - \gamma)Z_1^o(\tau) \tag{44}$$

An iterative procedure, comprising eq 34, 27, 43, 44, and 41 (solved in that order), now can be used to obtain a numerical solution. Iterations are required due to the dependence of R_s, R_o, $\mathcal{H}$, and $\exp(-A_r/\theta_r)$ on θ_r in this system of equations. θ_r from the preceding time step is utilized to start the solution for any new time step. The θ_r obtained at this new step is then successively iterated until its value converges. This provides a set of values of θ_r and τ and the corresponding oxide layer thicknesses ($Z_2^o - Z_1^o$).

Knowledge of θ_r at various τ [and, thereby, an estimate of $(d\theta_r/d\tau)$] will enable the calculation of temperature gradients across the Si–SiO_2 interface from eq 38 and 39.

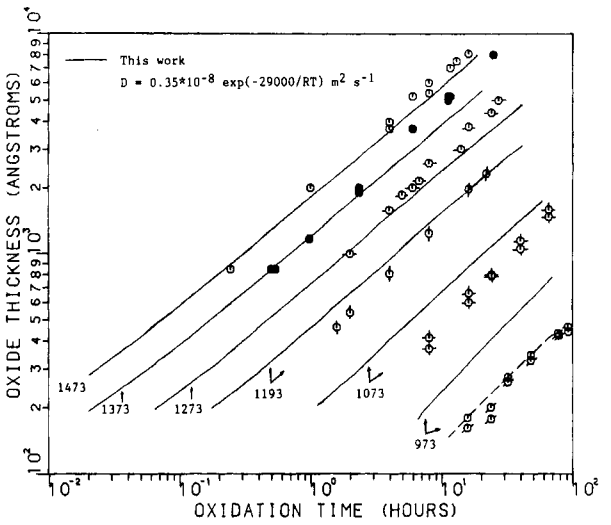

Figure 2. Oxidation of silicon in dry oxygen at various reactor temperatures (K); experimental data are from Deal and Grove (1965).

The corresponding temperature profiles in the two regions may now be obtained. For the oxide region, $\theta_o(z_o,\tau)$ may be numerically evaluated at various z_o between Z_1^o and Z_2^o from eq 29. Equation 37 for the silicon region, however, involves an integral which may be difficult to calculate, due to the nature of the $\theta_r - \tau$ data generated. This difficulty may be circumvented by fitting the $\theta_r - \tau$ data to a polynomial in τ as

$$\theta_r(\tau) - \sum_{n=0}^{N} a_n\tau^{n/2} \tag{45}$$

This polynomial expression (for an alternate form, see Carslaw and Jaeger (1959) and Crank (1975)) can then be used in eq 37 to yield, after integration,

$$\theta_s(z_s,\tau) = \sum_{n=0}^{N} a_n\Gamma\left(\frac{n}{2} + 1\right)(4\tau)^{n/2}i^n\,\mathrm{erfc}\left(\frac{Z_1^s - z_s}{2\eta(R_s\tau)^{1/2}}\right) + \theta_I\,\mathrm{erf}\left(\frac{Z_1^s - z_s}{2\eta(R_s\tau)^{1/2}}\right) \qquad 0 \leq z_s \leq Z_1^s \tag{46}$$

Γ in this expression is the gamma function. i^n erfc (x) are integral – erfc (x) functions with (see, e.g., Abramowitz and Stegun (1964)

$$\mathrm{ierfc}\,(x) = \frac{\exp(-x^2)}{\pi^{1/2}} - x\,\mathrm{erfc}\,(x) \tag{47a}$$

and the recurrence relation

$$i^n\,\mathrm{erfc}\,(x) = \frac{1}{2n}[i^{n-2}\,\mathrm{erfc}\,(x) - 2xi^{n-1}\,\mathrm{erfc}\,(x)] \tag{47b}$$

Results and Discussion

The simplified model, derived in the preceding section, has been numerically simulated to predict oxide growth and to determine if any significant temperature gradients were present across the Si–SiO_2 interface. The values of the physicochemical parameters employed in the simulation are given in the Appendix.

Results of the simulation of oxide growth are shown in Figure 2 for various reactor temperatures. The plots have been obtained under the assumption that, at time $t = 0$, the wafers are at a uniform temperature, equal to the reactor temperature [i.e., $\theta_s(z_s,0) = \theta_I(z_s) \equiv \theta_G$]. This assumption does not affect the results significantly since the time required to heat a thin wafer is very small compared

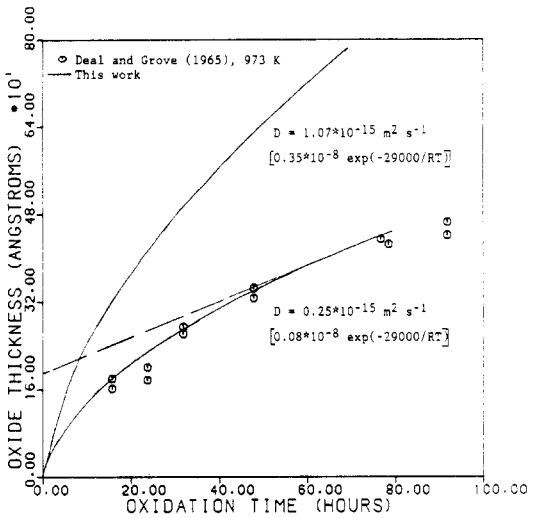

Figure 3. Oxidation of silicon in dry oxygen at 973 K; effect of diffusion coefficient employed in simulation.

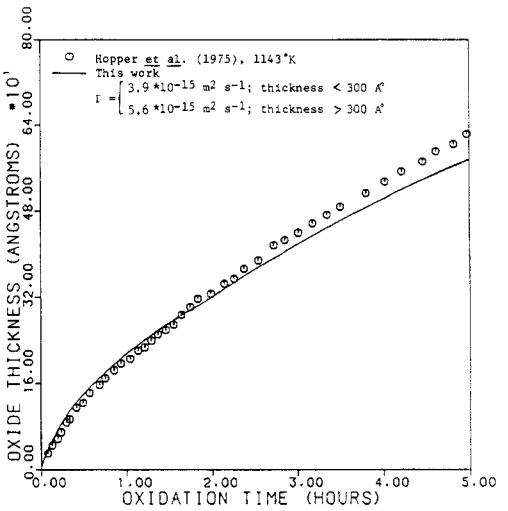

Figure 4. Oxidation of silicon in dry oxygen at 1143 K; initial oxidation period.

to the oxidation time. The results obtained from simulation are compared to experimental data from Deal and Grove (1965) in Figure 2. It is evident that the predicted values correspond quite well with the experimental data, especially at the higher oxidation temperatures. At lower temperatures (973–1073 K), the model, utilizing the given set of parameters, overpredicts the growth rate. A parametric study has indicated that the predicted values are most sensitive to the diffusivity. It is worth noting that this is the parameter with the greatest uncertainty. Large variations in preexponential factors and activation energies are reported, ranging from $2 \times 10^{-13} \exp(-29000/RT)$ m^2 s^{-1} (Williams, 1965) to $2.8 \times 10^{-8} \exp(-27000/RT)$ m^2 s^{-1} (Norton, 1961). Part of the discrepancy may be due to confusion about the mechanism of diffusion (for a review, see Tiller (1980a,b, 1981)). A separate simulation, using a diffusion coefficient reduced by a factor of 0.25, has been conducted for oxidation at 973 K. The result is illustrated in Figure 3 along with the experimental data. The figure exhibits a good fit to the experimental data.

During dry oxidation, an initial period of rapid oxidation is observed. This period is explained on the basis of rapid ionic oxygen transport until the oxide thickness becomes large compared to the extent of the space–charge region within the oxide. The transport mechanism reverts to molecular transport beyond this space–charge region. The extent of this region is estimated to be between 150 and 250 Å (Deal and Grove, 1965). This explanation has been disputed by Blanc (1978) who has suggested that the rapid oxidation regime is not an "anomaly". He has proposed that, while oxygen diffuses as a molecule, the actual oxidant is atomic oxygen. Blanc has revised the original model of Deal and Grove to describe the oxidation data up to 2000 Å.

The model presented herein is able to adequately describe this initial period. This is evident in Figure 3 where the linear growth period extrapolates back to a thickness of 185 Å at $t = 0$. A more precise set of low reaction time oxidation data, obtained by Hopper et al. (1975) at 1143 K, has been modeled in Figure 4. A reasonable fit is obtained, employing slightly different diffusion coefficients, above and below 300 Å. This is consistent with the change in transport mechanism discussed in the previous paragraph.

A $Si–SiO_2$ interface having a finite thickness could be included in the model by replacing the boundary conditions at X_1 (eq 4, 8, 11, 22, 24, and 26) with mass- and heat-transport equations describing a transition region between Si and SiO_2. Definition of arbitrary interfaces between the Si, SiO_2, and transition regions woul be required, as would initial and boundary conditions at these interfaces. However, the estimated system parameters from experimental data (Deal and Grove, 1965) show that the reaction rate is at least 2 orders of magnitude faster than both the oxide film growth rate and the diffusive mass-transfer rate. This demonstrates that reaction between the oxidizing species and the silicon occurs at rates sufficient for the reaction at the interface to be completed before diffusion of the oxidizing species into the silicon can occur. The result is effectively an interface of negligible thickness and considerable simplification of the governing equations.

The values of $[d\theta_r/d\tau]$ and $[\partial\theta_s/\partial z_s]_{Z_1^s}$, obtained in the present simulations indicate that the system does not deviate from isothermal conditions. $[d\theta_r/d\tau]$ ranges from 10^{-6} to 10^{-16} K s^{-1}, while $[\partial\theta_s/\partial z_s]_{Z_1^s}$ varies between 10^{-5} and 10^{-12} K m^{-1}. These values are consistent with the fact that the reaction is highly exothermic. However, the rate of reaction is low and extensive time periods are required for complete oxidation. Therefore, uniform temperature profiles, each equal to the particular reactor temperature, are obtained (eq 29 and 46 for $\theta_r(\tau) = \theta_o(Z_2^o,\tau) \equiv \theta_G$). It can thus be concluded that stresses in the silicon wafer, due to thermal mismatch, are primarily generated during the cooling down process.

Conclusions

A rigorous one-dimensional model for the dry oxidation of silicon, taking into account both mass and heat transfer, has been derived. Simplifications, based on order of magnitude arguments, have been made to obtain an analytic solution of the governing equations of the model. However, isothermal behavior of the system is not assumed. In addition, the moving $Si–SiO_2$ boundary of the oxidation system is included.

The solution has been numerically simulated to predict the growth rate of the oxide layer and the temperature profiles in the system. The predicted rate of oxide layer growth agrees reasonably well with experimental data. The predicted values are highly sensitive to the value chosen for the diffusion coefficient. This model has been used to fit the available oxide growth data from a variety of sources over a temperature range from 973 to 1473 K. In addition, the model describes rates for oxide layer growth during the

initial period of rapid oxidation (film thicknesses of less than 250 Å).

Acknowledgment

Presented at the symposium on Modern Applications of Chemical Engineering Theory, AIChE 1987 spring meeting, March 29–April 2, Houston, TX (Paper 55f). This work was conducted under the sponsorship of the Engineering Experiment Station, Kansas State University, Manhattan, KS 66506.

Nomenclature

a_n = polynomial coefficients defined in eq 45
C = concentration of unreacted oxygen in the oxide layer, mol m^{-3}
C^* = saturation solubility of unreacted oxygen at the SiO_2–boundary layer interface in equilibrium with the ambient or reactor atmosphere, mol m^{-3}
C^*_{ref} = saturated solubility of unreacted oxygen in silicon dioxide in equilibrium with ambient atmosphere at T_{ref} [$\equiv C^*(T_{ref})$], mol m^{-3}
C_{pg} = heat capacity of oxygen, cal kg^{-1} K^{-1}
C_{ps} = heat capacity of silicon, cal kg^{-1} K^{-1}
C_{po} = heat capacity of silicon dioxide, cal kg^{-1} K^{-1}
D = diffusivity of molecular oxygen in SiO_2, m^2 s^{-1}
D_0 = preexponential factor for diffusivity, m^2 s^{-1}
E = activation energy for reaction, cal mol^{-1}
E_d = activation energy for diffusion, cal mol^{-1}
h_m = boundary layer mass-transfer coefficient, m s^{-1}
h_t = boundary layer heat-transfer coefficient, cal m^{-2} s^{-1} K^{-1}
ΔH = heat of reaction, cal mol^{-1}
k = preexponential factor for reaction rate constant, m s^{-1}
k'' = reaction rate constant, m s^{-1}
K_o = thermal conductivity of silicon dioxide, cal m^{-1} s^{-1} K^{-1}
K_s = thermal conductivity of silicon, cal m^{-1} s^{-1} K^{-1}
M_g = molecular weight of oxygen, daltons
M_o = molecular weight of silicon dioxide, daltons
M_s = molecular weight of silicon, daltons
R = gas constant, cal mol^{-1} K^{-1}
t = time, s
T_G = ambient or reactor temperature, K
T_I = initial temperature distribution in wafer, K
T_o = temperature in the oxide layer, K
T_r = temperature of reaction at the Si–SiO_2 interface, K
T_{ref} = reference temperature, K
T_s = temperature in the silicon layer, K
V_o = convective velocity for heat transfer in the oxide region, m s^{-1}
V_1 = velocity of the Si–SiO_2 interface, m s^{-1}
V_2 = velocity of the SiO_2–boundary layer interface, m s^{-1}
x = position, spatial coordinate, m
X_1 = position of the Si–SiO_2 interface, m
X_2 = position of the SiO_2–boundary layer interface, m

Greek Symbols

δ = original half-thickness of wafer, m
δ_o = representative thickness of the oxide layer employed for nondimensionalization, m
ρ_o = density of silicon dioxide, kg m^{-3}
ρ_s = density of silicon, kg m^{-3}

Dimensionless Groups

$A_d = E_d/RT_{ref}$, activation energy for diffusion
$A_r = E/RT_{ref}$, activation energy for reaction
$H = |\Delta H|kC^*_{ref}\delta_o/K_oT_{ref}$, heat of reaction
$R_o = K_o/(\rho_oC_{po}D_0)$
$R_s = K_s/(\rho_sC_{ps}D_0)$
$R_{so} = K_s/K_o$, ratio of thermal conductivities
$Nu_{ho} = h_t\delta_o/K_o$, Nusselt number for heat transfer
$Nu_m = h_m\delta_o/D_0$, Nusselt number for mass transfer
$S_r = k\delta_o/D_0$
$U_o = [dZ_2^o/d\tau] + W_g\{-(\exp(-A_d/\theta_o))\ \partial y/\partial z_o + [dZ_2^o/d\tau]y\}$
$W = M_sC^*_{ref}/\rho_s$
$W_g = M_gC_{pg}C^*_{ref}/\rho_oC_{po}$
$y = C/C^*_{ref}$, unreacted oxygen concentration in the oxide layer
$y^* = C^*(T_o|_{Z_2^o})/C^*_{ref}$, equilibrium unreacted oxygen concentration at the SiO_2–boundary layer interface
$z_o = x/\delta_o$, $X_1^+ \leq x \leq X_2^-$
$z_s = x/\delta_s$, $0 \leq x \leq X_1^-$
$Z_1^o = X_1/\delta_o$, position of the Si–SiO_2 interface
$Z_2^o = X_2/\delta_o$, position of the SiO_2–boundary layer interface
$Z_1^s = X_1/\delta$, position of the Si–SiO_2 interface

Dimensionless Greek Symbols

$\alpha_o = K_o/\rho_oC_{po}$, thermal diffusivity of silicon dioxide
$\alpha_s = K_s/\rho_sC_{ps}$, thermal diffusivity of silicon
$\gamma = (\rho_s/M_s)/(\rho_o/M_o)$
$\eta = \delta_o/\delta$, ratio of dedimensionalizing factors
$\theta_G = T_G/T_{ref}$, reactor or ambient temperature
$\theta_I = T_I/T_{ref}$, initial temperature distribution in wafer
$\theta_o = T_o/T_{ref}$, temperature in the oxide layer
$\theta_r = T_r/T_{ref}$, temperature of reaction at the Si–SiO_2 interface
$\theta_s = T_s/T_{ref}$, temperature in the silicon layer
$\tau = tD_0/\delta_o^2$, Fourier time

Appendix. Physicochemical Parameters of the Si-SiO_2 System

Densities (neglecting thermal expansion), kg m^{-3}

$$\rho_s = 2330 \qquad \rho_o = 2250$$

Heat capacities, kcal kg^{-1} K^{-1} (Barin and Knacke, 1973)

$$C_{ps} = 0.1942 + 3.282 \times 10^{-5}T_s - 3.012 \times 10^3/T_s^2$$

$$C_{po} = 0.1747 + 15.438 \times 10^{-5}T_o - 3.849 \times 10^3/T_o^2 \qquad T_o < 847\ K$$

$$C_{po} = 0.2343 + 3.994 \times 10^{-5}T_o \qquad T_o > 847\ K$$

Thermal conductivities, kcal m^{-1} s^{-1} K^{-1}

$$K_s = 0.0358 \qquad K_o = 2.6 \times 10^{-4}$$

Boundary layer mass-transfer coefficient, m s^{-1} (Deal and Grove, 1965)

$$h_m = 2.8$$

Boundary layer heat-transfer coefficient, kcal m^{-2} s^{-1} K^{-1}

$$h_t = 0.1$$

Diffusivity of molecular oxygen in SiO_2, m^2 s^{-1} (Deal and Grove, 1965; Kofstad, 1972)

$$D = (0.08 - 0.35) \times 10^{-8} \exp(-29000/RT_o)$$

Saturation solubility of oxygen on the SiO_2 surface, mol m^{-3} (estimated from Deal and Grove (1965))

$$C^* = 2.55 \times 10^{-1} \exp(-2737.5/RT_o|_{X_2})$$

Rate coefficient for reaction, m s^{-1} (estimated from Deal and Grove (1965))

$$k'' = 6640.9 \exp(-40345.87/RT_r)$$

Heat of reaction, kcal mol^{-1} (calculated from Barin and Knacke (1973))

$$10^3\Delta H = -2.119T_r + 3.677 \times 10^{-3}T_r^2 + 1.067 \times 10^5/T_r - 217753.16 \qquad T_r < 847\ K$$

$$10^3\Delta H = 1.465T_r + 0.239 \times 10^{-3}T_r^2 - 1.246 \times 10^5/T_r - 210618.15 \qquad T_r > 847\ K$$

Registry No. Si, 7440-21-3; SiO_2, 7631-86-9.

Literature Cited

Abramowitz, M.; Stegun, I. A. *Handbook of Mathematical Functions With Formulas, Graphs, and Mathematical Tables*; Applied Mathematics Series 55; National Bureau of Standards: Washington, DC, 1964; p 299.

Barin, I.; Knacke, O. *Thermochemical Properties of Inorganic Substances*; Springer-Verlag: Berlin, 1973; p 689.

Bird, R. B.; Stewart, W. E.; Lightfoot, E. N. *Transport Phenomena*; Wiley: New York, 1960; pp 352-353.

Blanc, J. *Appl. Phys. Lett.* **1978**, *33*, 424-426.

Carslaw, H. S.; Jaeger, J. C. *Conduction of Heat in Solids*; Clarendon: Oxford, 1959; pp 62-63.

Crank, J. *Q. J. Mech. Applied Math.* **1957**, *X*, 220-231.

Crank, J. *The Mathematics of Diffusion*; Clarendon: Oxford, 1975; pp 32-34.

Deal, B. E.; Grove, A. S. *J. Appl. Phys.* **1965**, *36*, 3770-3778.

Dutton, R. W.; Antoniadis, D. A. In *Moving Boundary Problems*; Wilson, D. G., Solomon, A. D., Boggs, P. T., Eds.; Academic: New York, 1978; pp 233-248.

Ghandhi, S. K. *VLSI Fabrication Principles*; Wiley: New York, 1983; pp 370-400.

Hopper, M. A.; Clarke, R. A.; Young, L. *J. Electrochem. Soc.* **1975**, *122*, 1216-1222.

Katz, L. E. In *VLSI Technology*; Sze, S. M., Ed.; McGraw-Hill: New York, 1983; pp 131-167.

Kofstad, P. *Nonstoichiometry, Diffusion and Electrical Conductivity in Binary Metal Oxides*; Wiley-Interscience: New York, 1972; pp 348-355.

Lane, C. H. *IEEE Trans. Electronic Devices* **1968**, *ED-15*, 998-1003.

Norton, F. J. *Nature (London)* **1961**, *191*, 701.

Rubinstein, L. I. *The Stefan Problem*; American Mathematical Society: Providence, RI, 1971; pp 52-55.

Singh, S. K.; Fan, L. T. *Biotechnol. Prog.* **1986**, *2*, 145-156.

Talman, Y.; Davis, H. T.; Scriven, L. E. *AIChE J.* **1981**, *27*, 928-937.

Tao, L. C. *AIChE J.* **1967**, *13*, 165-169.

Tiller, W. A. *J. Electrochem. Soc.* **1980a**, *127*, 619-624.

Tiller, W. A. *J. Electrochem. Soc.* **1980b**, *127*, 625-632.

Tiller, W. A. *J. Electrochem. Soc.* **1981**, *128*, 689-697.

Wen, C. Y. *Ind. Eng. Chem.* **1968**, *60*, 34-54.

Williams, E. L. *J. Amer. Ceramic Soc.* **1965**, *48*, 190-194.

Wilmsen, C. W.; Thompson, E. G.; Meissner, G. H. *IEEE Trans. Electronic Devices* **1972**, *ED-19*, 122.

Yariv, A. *An Introduction to Theory and Applications of Quantum Mechanics*; Wiley: New York, 1982; pp 253-259.

Received for review October 23, 1987
Revised manuscript received April 29, 1988
Accepted May 17, 1988

Correlation and Prediction of Physical Properties of Hydrocarbons with the Modified Peng-Robinson Equation of State. 1. Low and Medium Vapor Pressures

B. Carrier, M. Rogalski, and A. Péneloux*

Laboratoire de Chimie-Physique, Faculté des Sciences de Luminy, 13228 Marseille, Cedex 9, France

A modified version of the Peng-Robinson equation of state is proposed for representing vapor pressure data on compounds currently encountered in petroleum fractions. The proposed equation is valid from the triple point up to 2-3 bar. When one parameter is adjusted using experimental data, a very accurate representation of vapor pressures is obtained, with an overall average absolute deviation of only 0.19% in the case of the 128 substances studied. When this parameter was determined by using a group contribution method, the corresponding deviation was 0.43%.

Vapor pressures of pure compounds can be calculated either from some integrated forms of the Clausius-Clapeyron equation or from an equation of state. The first method is currently used to precisly represent experimental vapor pressure data. Numberous expressions proposed in the literature represent experimental data with a good degree of accuracy, but they are often disappointing when used for extrapolation purposes (especially in the very low pressure range). By using the corresponding states principle with expressions of this type, it is possible to obtain general, predictive equations for calculating the vapor pressure of a given compound on the basis of a set of characteristic parameters (usually critical constants and the acentric factor). Results obtained are satisfactory in the high-pressure range and usually only roughly correct at medium (0.06-3 bar) and low pressures (less than 0.06 bar). As examples, the papers by Gomez-Nieto and Thodos (1977), Riedel (1954), Thek and Stiel (1966), and Willman and Teja (1985) can be quoted.

Equations of state are usually used as a means of calculating volumetric and thermal properites of pure compounds and mixtures as well as phase equilibria. Thus, it is necessary that they represent the vapor pressures with a good degree of accuracy. Their parameters are usually scaled in terms of the corresponding states principle, i.e., using critical parameters and the acentric factor.

If we consider the family of cubic equations of state, the general form is given as

$$P = RT/(v - b) - a/(v^2 + ubv + wb^2) \quad (1)$$

Matching an equation of state of this type with vapor pressures means fitting the parameter a of eq 1 to experimental data. The quality of the fitting depends on the expression chosen to represent variations in parameter a with temperature.

An expression currently used was proposed by Soave (1972):

$$a(T) = a_c(1 + m_s(1 - T_r^{1/2}))^2 \quad (2)$$

By means of eq 2 or its modifications proposed in the literature together with one of the forms of eq 1, it is possible to calculate the vapor pressures of hydrocarbons quite correctly in the high-pressure range. At medium pressures (0.06-3 bar), the representation is still fairly correct (Rauzy, 1982) but is far from being as accurate as experimental data. The main advantage of an equation of state of this type when applied to vapor pressure calculations is its predictive character. It is possible to improve the restitution of vapor pressures by defining the parameter $a(T)$ of eq 1 with more characteristic parameters per compound than in the case of eq 2. This approach was developed recently by Gibbons and Laughton (1984)

0888-5885/88/2627-1714$01.50/0

ADDITIONS AND CORRECTIONS

Modeling of Thermal Oxidation of Silicon [Volume 27, Number 9, page 1707]. Satish K. Singh, John R. Schlup,* L. T. Fan, and Biswajit Sur

Page 1711. Equation 40 should read as follows:

$$\frac{d\theta_r}{d\tau}\left\{-2R_{so}\left(\frac{\tau}{\pi R_s}\right)^{1/2}\right\} - \theta_r\left\{\frac{Nu_{ho}}{1 + Nu_{ho}(Z_2^\circ - Z_1^\circ)} + \left(\frac{R_{so}}{R_s} - \frac{1}{R_o}\right)\left[\frac{dZ_1^\circ}{d\tau}\right]\right\} + \left\{\frac{\theta_G Nu_{ho}}{1 + Nu_{ho}(Z_2^\circ - Z_1^\circ)} + [H \exp(-A_r/\theta_r)y]_{Z_1^\circ}\right\} = 0 \quad (40)$$

Page 1711. Equation 45 should read as follows:

$$\theta_r(\tau) = \sum_{n=0}^{N} a_n \tau^{n/2} \quad (45)$$